Available online at www.sciencedirect.com
ScienceDirect
Ceramics International 37 (2011) 3265–3271
CERAMICS INTERNATIONAL
www.elsevier.com/locate/ceramint

In vitro properties of nano-hydroxyapatite/chitosan biocomposites

Khaled R. Mohamed [a,*], Zenab M. El-Rashidy [a], Aida A. Salama [b]

[a] Biomaterials Dept., National Research Centre, Dokki, Cairo, Egypt
[b] Biophysics Dept., Faculty of Science, Al-Azhar University, Cairo, Egypt

Received 18 March 2011; received in revised form 13 May 2011; accepted 23 May 2011
Available online 27 May 2011

Abstract

In vitro behavior of the composites was performed in simulated body fluid (SBF) to induce the formation of bone-like apatite layer onto their surfaces and its enhancement in the presence of citric acid (CA). The results proved the mineralization of calcium (Ca^{2+}) and phosphorus (P) ions onto the composites which contain high chitosan concentration especially after longer time of immersion. The degradation data decreased with increase chitosan content especially C2 composites (containing 30% chitosan) and highly decreased in the presence of CA which increased binding strength through the composite. The swelling % increased with increase of chitosan content in HA composite but it decreased with CA addition as increase of interaction between three matrices. The Fourier Transformed Infrared Spectroscopy (FT-IR) and Scanning Electron Microscope (SEM-EDAX) confirmed the formation of bone-like apatite layer on the surface of the composites especially these containing CA. These biocomposites have unique in vitro properties for bone substitute's applications in the future.

Keywords: B. Composites; Chitosan; Hydroxyapatite; In vitro; SEM

1. Introduction

Every year, millions of patients, particularly among the aged, are suffering from bone defects arising from trauma, tumor or bone disease and of course several are dying due to insufficient ideal bone substitute. The composites of ceramics with natural degradable polymers have attracted much interest as bone filler. These biocomposites represent a system which contains the specific features for HA and biopolymer material similar to bone structure, which is composed of calcium, phosphate salts and collagen fiber [1]. Hydroxyapatite has history of being used as a biomaterials in bone grafting, bone tissue engineering, and drug delivery, owing to its obvious properties of biocompatibility, bioactivity, osteoconductivity, non-toxicity, non-inflammatory and non-immunogenicity [2]. Although HA is considered as a good bone substitute, HA ceramic slightly differs from the biological apatite in terms of structure, composition, crystallinity, solubility, and biological reactivity. The presence of CO_3^{2-} ions into HA ceramic plays a vital role in the bone metabolism and they occupy about 8 wt% of the calcified tissue and may vary depending on the age factor [3].

Chitosan is obtained by a full or partial deacetylation of chitin, a very abundant natural polymer derived from the shells of crustacean, it has numerous and interesting biological properties such as biocompatibility, biodegradability and non toxic properties, chitosan becomes one of the most useful polysaccharides in biomedical area [4]. Chitosan has been used in combination with materials to enhance bone growth such as bone filling pastes [5]. The chitosan scaffold degraded in phosphate buffer saline containing lysozyme after 4 weeks and the pH of incubation media indicated acidic condition [6]. The swelling property is one of the prime factors to contribute to biocompatible nature of synthetic biomaterials and it is the amount of water content which imparts several physicochemical properties to the materials [7]. Chitosan material is known to swell in aqueous solution and sometimes, this property can be used to secure biomaterials inside the implanted space [8].

The chitosan in HA\chitosan composite gradually degraded during the soaking in SBF solution, which resulted in plenty of macro- and micro-pores on the surface and inside the specimens. At the same time, a lot of tiny apatite crystals deposited on the surface of the specimens. At the first 4 weeks, the degradation rate of chitosan was higher than the deposition

* Corresponding author.
E-mail address: kh_rezk1966@yahoo.com (K.R. Mohamed).

0272-8842/$36.00
doi:10.1016/j.ceramint.2011.05.121

Table 1
Preparation of nHA/chitosan composites (C composites).

Samples	HA/chitosan composition (weight ratio)	$Ca(OH)_2$ (g)	H_3PO_4 (g)	Chitosan (g)
HA powder	100/0	14.76	11.71	0.00
C1 comp.	80/20	11.81	9.37	4.00
C2 comp.	70/30	10.33	8.20	6.00
C3 comp.	60/40	8.86	7.03	8.00

rate of apatite on the surface of specimens. After that, the deposition of apatite is prior to the degradation of chitosan, so the rate of weight loss decreased [9]. The swelling of HA\chitosan composite scaffold in physiological saline medium indicated 88% swelling in 1 h and afterwards no further change in the constituents of the composite materials [8]. The SEM for HA\chitosan composite shows the rough surface which increases with n-HA content and some small irregular pores appear on the surface of composite. The roughness and pores on the surface are essential for cells adhesion and crawl, and will also promote the growth of cells [10].

Citric acid ($C_6H_8O_7$) has a hydroxyl and three carboxyl groups in its molecules. Citric acid also found in bone in the form of citrate in 0.9 wt% [11]. Since the citric acid has a strong chelating ability of calcium ions to its carboxylate groups, it is believed to induce HA nucleation in 1.5 SBF solutions [12]. Therefore, citric acid was used as a nucleating agent for HA crystals on cellulose material in SBF. The hydroxyl groups of CA can bind to hydroxyl group of cellulose through hydrogen bonding and can induce the HA particles on it [13]. A key feature for CA-derived biomaterials is that CA provides valuable pendant functionality participating in the ester bond-crosslink formation, enhancing hemcompatibility, balancing the hydrophilicity of the polymer network, and providing hydrogen bonding [14].

The potential bioactivity of the material being evaluated by the in vitro studies is much cheaper and quicker than in vivo studied. From this point of view, in the present study, we are concerning with the effect of CA on formation of carbonated apatite layer onto nHA/chitosan composites in SBF solution. The different measurements such as Ca^{2+} and P ions in SBF, degradability, swelling, FT-IR and microstructure analysis for solid composites after withdrawal from SBF were performed to confirm the formation of apatite layer onto their surfaces and its enhancement in the presence of CA.

2. Materials and methods

2.1. Materials

The starting materials for preparing hydroxyapatite (HA) is calcium hydroxide ($Ca(OH)_2$) (BDH) and orthophosphoric acid (H_3PO_4) (85%) (Laboratory Rasayan). Other materials were chitosan polymer (viscosity 800 cps) with high molecular weight (M_r = 600,000) and deacetylation (85%) (Sigma–Aldrich), citric acid (CA) (anhydrous) (Morgan Chemical Ind. Co., Egypt), ethanol (E) and acetic acid (96%) (EL-Nasr Pharmaceutical Co., Egypt).

2.2. Methods

2.2.1. Preparation

Table 1 shows the C composites with different weight ratios of HA and chitosan polymer and were prepared according to Li et al. [1]. The C2 composite with weight ratio composition [(HA: chitosan (70:30)] was prepared as follows: the chitosan solution with a concentration of 6% prepared by dissolving chitosan (6 g) into 2% AA with stirring for 5 h to get a perfectly transparent solution. Then, the solution was mixed with 8.20% solution of H_3PO_4 and dropped slowly into the 10.33% ethanol solution of Ca $(OH)_2$ with vigorous stirring kept for 24 h after dropping and then the paste obtained was aged for another 24 h. Finally, the precipitate was filtered, washed with distilled water to remove the excess NaOH solution and dried in a vacuum oven at 70 °C. The chitosan polymer was dissolved in 0.2 M citric acid solution instead of 2% AA. After that, the above steps were repeated to prepare C·CA composites with different weight ratios of HA and chitosan polymer (Table 1). The prepared composites were mentioned for in vitro test and are shown in Table 2.

2.2.2. In vitro behavior

2.2.2.1. Solution analysis. The composites samples were weighed and immersed in certain volume of SBF which proposed by Kokubo and Takadama [15]. The SBF has a composition similar to human blood plasma and has been extensively used for in vitro test. The experiments carried out at the body temperature (37 °C) and pH: 7.4 for different periods up to 28 days. The calcium and phosphorus ions were measured pre- and post-immersion in SBF. After the immersion periods end, the solution were analyzed by spectrophotometer (UV-2401PC, UV–VIS Recording spectrophotometer, Shimadzu,

Table 2
Notation of the composites used in the present work.

C1 composite	80%HA/20% chitosan composite
C1·CA composite	80%HA/20% chitosan composite containing 0.2 M citric acid solution
C2 composite	70%HA/30% chitosan composite
C2·CA composite	70%HA/30% chitosan composite containing 0.2 M citric acid solution
C3 composite	60%HA/40% chitosan composite
C3·CA composite	60%HA/40% chitosan composite containing 0.2 M citric acid solution

Japan) using biochemical kits (Techno Diagnostic, USA) to measure the total calcium ions at λ = 570 nm and phosphorus ions concentration at λ = 675 nm. Each test was repeated 3 times and the average value was taken to confirm the results [16].

2.2.2.2. Assessment of composites

2.2.2.2.1. Degradation test (D%). The degradation test of the composites was carried in vitro by incubating the composite in SBF at pH: 7.4 and 37 °C for different periods (1, 3, 7, 15, 21 and 28 days). At interval time, the composites were taken from the medium and dried at 50 °C over night. The degradable ratio (*D%*) was examined by weight loss from the following formula according to [17].

$$D\% = \frac{W_o - W_i}{W_o} \times 100$$

where W_o denotes the original weight, while W_i is the weight at time (t). Each experiment was carried out for the 3 samples and the average values were taken to confirm the results.

2.2.2.2.2. Swelling test (S%). For water uptake measurements, all the specimens were weighted before being immersed in distilled water. After immersion for different periods, the samples were carefully removed from the medium and gently pressed in-between two filters paper to remove excess water and finally weighted using a sensitive balance. Water absorption (Swelling %) is given using the following equation:

$$S\% = \frac{W_f - W_i}{W_i} \times 100$$

where W_i is the initial weight of the sample, and W_f is the sample weight after immersion. The experiment was carried out for the 3 samples and the average value was taken to ensure the result.

2.2.2.2.3. FT-IR analysis. The FT-IR analysis was used to assess the composites pre- and post-immersion in SBF for different periods. The range of wave-number used was 4000–400 cm^{-1} with normal slit. The available computerized infrared spectrometer (Jasco, FT/IR 300E, Fourier Transform Infrared Spectrometer, Serial No. 4140109, and Japan) was used in this study.

2.2.2.2.4. Microstructure analysis. The surface morphology of the composites specimens was studied using SEM, JXA 840A Electron Probe Microanalyzer (JEOL, Japan). For SEM, the substrates were mounted on metal stubs and coated with gold before being examined. Also, X-ray elemental analysis (EDAX) was carried out to some composites post-immersion to know the concentration of calcium and phosphorus elements on the surface for confirming the formation of apatite layer.

3. Results and discussion

3.1. In vitro behavior

The SBF solution and composites were assessed pre- and post-immersion in SBF for different periods to verify the formation of apatite materials onto their surfaces.

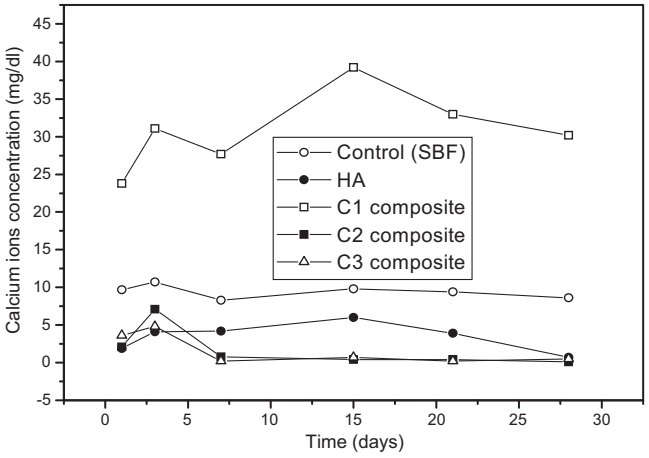

Fig. 1. The concentration of calcium ions for C composites compared to control (SBF) and HA sample for different periods. Standard error ($n = 3$) ±0.409.

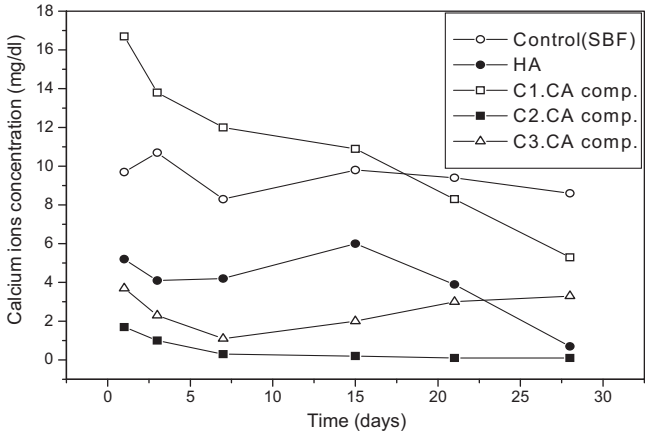

Fig. 2. The concentration of calcium ions for C·CA composites compared to control (SBF) and HA sample for different periods, Standard error ($n = 3$) ±0.384.

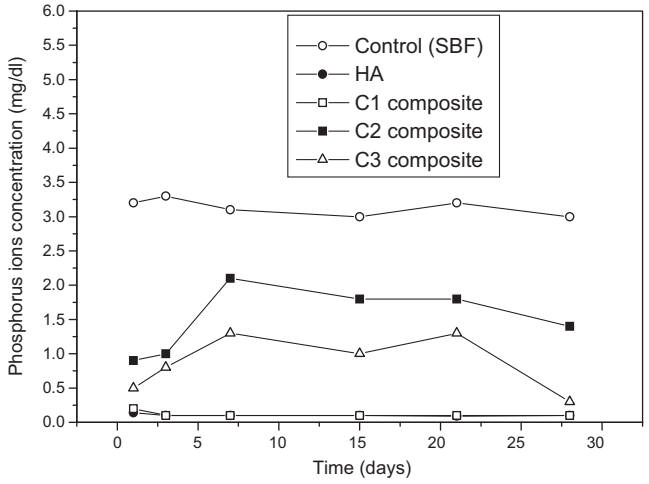

Fig. 3. The concentration of phosphorus ions in SBF post-immersion of C composites for different periods compared to control (SBF) and HA sample. Standard error ($n = 3$) ±0.209.

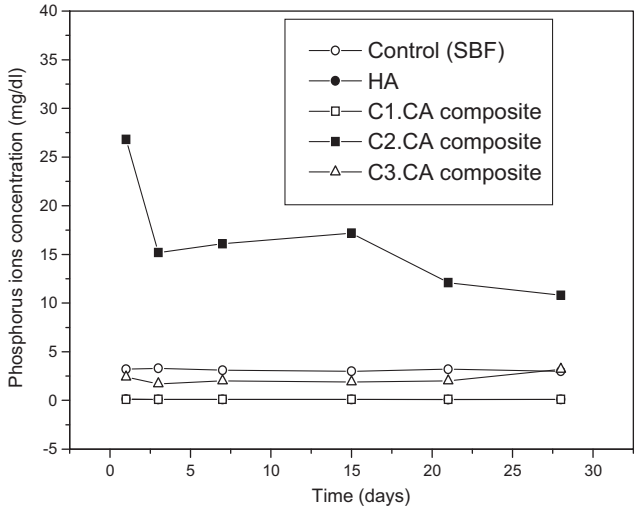

Fig. 4. The concentration of phosphorus ions for C·CA composites compared to control (SBF) and HA sample for different periods. Standard error ($n = 3$) ±0.309.

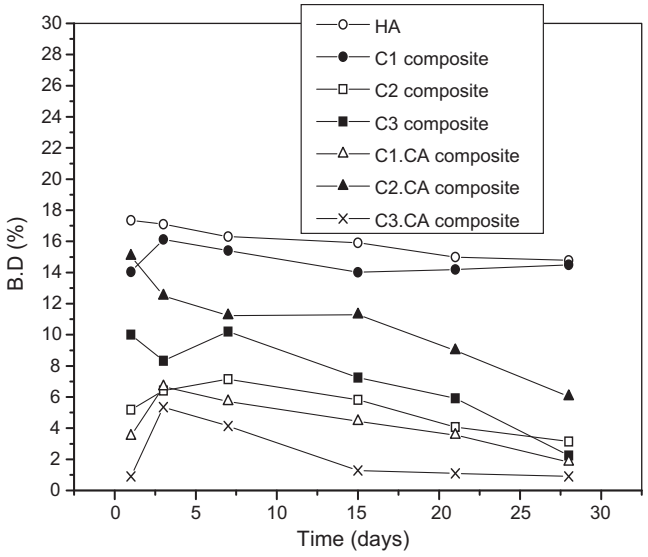

Fig. 5. The degradation % of C and C·CA composites compared to HA sample.

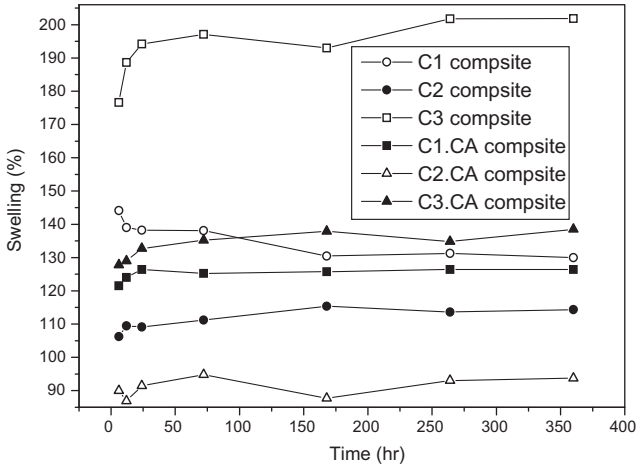

Fig. 6. The swelling % of C and C·CA composites in distilled water at 37 °C.

3.1.1. Solution analysis

3.1.1.1. Calcium ions (Ca^{2+}). The concentration of Ca^{2+} ions reduced in SBF for HA sample, C2 and C3 composites compared to control proving deposition of Ca^{2+} ions onto their

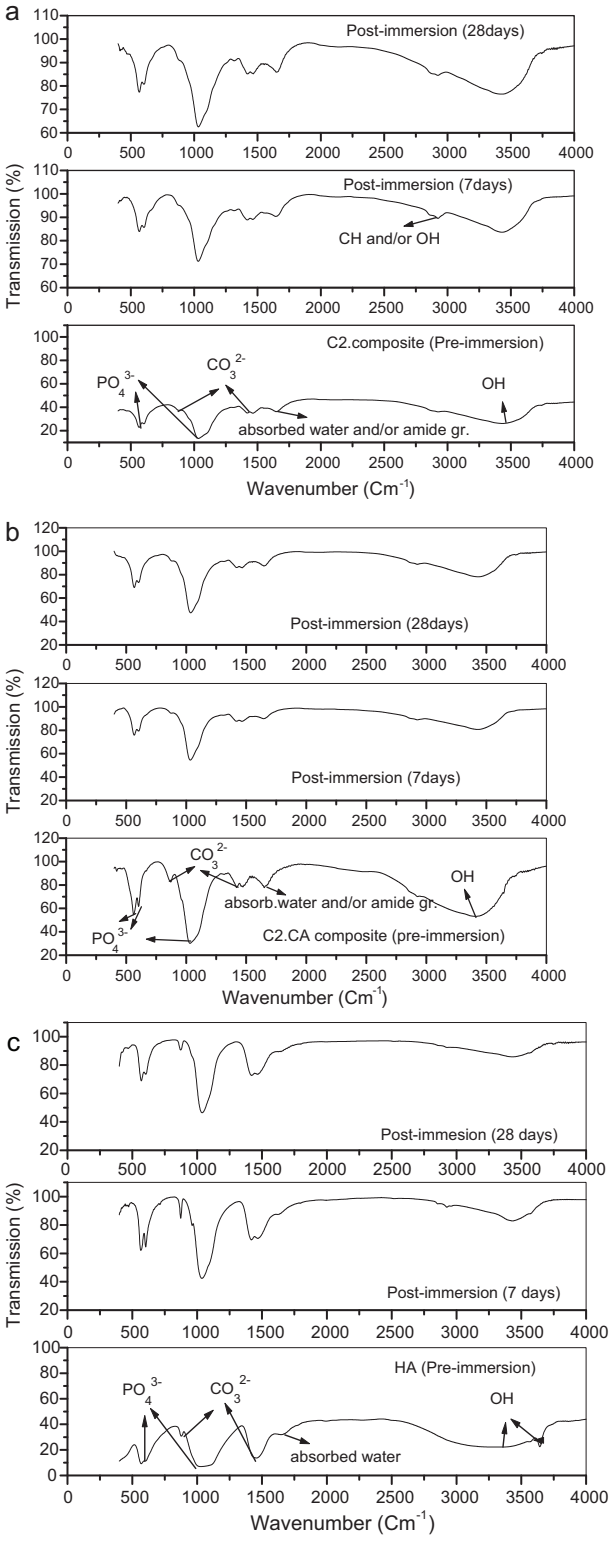

Fig. 7. (a) The FT-IR of HA sample pre- and post-immersion in SBF. (b) The FT-IR of C2 composite pre- and post-immersion in SBF. (c) The FT-IR of C2·CA composite pre- and post-immersion in SBF.

surfaces because of interaction between amino groups of chitosan and OH and Ca^{2+} of SBF. For C1 composite, concentration of Ca^{2+} ions increased compared to the control and the other samples due to the highest concentration of HA which had amorphous structure and high solubility (Fig. 1). On the other hand, the concentration of Ca^{2+} ions reduced in SBF for HA and C·CA composites compared to the control and C composites proving enhancement of the mineralization of Ca^{2+} ions onto the composite surface because of addition of CA which characterizes chelating of calcium ions from SBF [18] (Fig. 2).

3.1.1.2. Phosphorous ions (P). The concentration of P ions post-immersion recorded lower values for HA and C composites compared to control proving deposition of P ions onto their surfaces (Fig. 3). In this context, this result could be due to the affinity of chitosan as cationic polymer to phosphate ions in SBF [16,17]. On the other hand, the concentration of P ions post-immersion recorded lower values for HA, C1·CA and C3·CA composites compared to control proving deposition of P ions onto their surfaces (Fig. 4). It was reported that citric acid had less effect on chitosan than HA, probably through electrostatic interactions or the formation of chitosan–citrate complex, because of CA contains carboxyl group >2, which forms negative charged complex, that binds to NH^{3+} of the chitosan [19].

3.1.2. Assessment of composites

3.1.2.1. Degradation test (D%). The *D%* of HA is higher than all C and C·CA composites proving amorphous structure of nano-HA characterizing higher solubility. By increasing the chitosan content, the D% decreased for all composites especially the composite containing CA compared to HA (Fig. 5). This result is due to CA improved interaction between HA particles and chitosan, and increased the apatite formation causing reduction of chitosan degradation [9].

3.1.2.2. Swelling test (S%). The *S%* increased with increasing soaking time and chitosan concentration until reach to the highest value for C3 composite which contains the highest content of chitosan characterizing hydrophilic properties. While, the increase of HA powder into the composite decreased *S%* for all C composites as in C1 composite due to the formation of a temporary HA barrier preventing water permeating into the chitosan matrix [20]. On the other hand, the *S%* of C·CA composites recorded lower values compared to C composites (Fig. 6). This result is due to the OH of chitosan interacts with OH groups of HA or CA leading to reduction of free OH content in C·CA composites, then reduced hydrophilic properties for all C composites.

3.1.2.3. FT-IR analysis. The FT-IR show that the intensity of HA bands such as OH, phosphate and carbonate groups appeared at (3650 and 3400 cm^{-1}), (570 and 1030 cm^{-1}) and (880 and1450 cm^{-1}), respectively, in HA spectrum increased post-immersion at 7 and 28 days compared to pre-immersion proving biolayer apatite formation (Fig. 7a). For C2 composite, the intensity of the same HA bands in spectrum of C2 composite increased post-immersion at 7 and 28 days compared to pre-immersion as a result of high chitosan content which

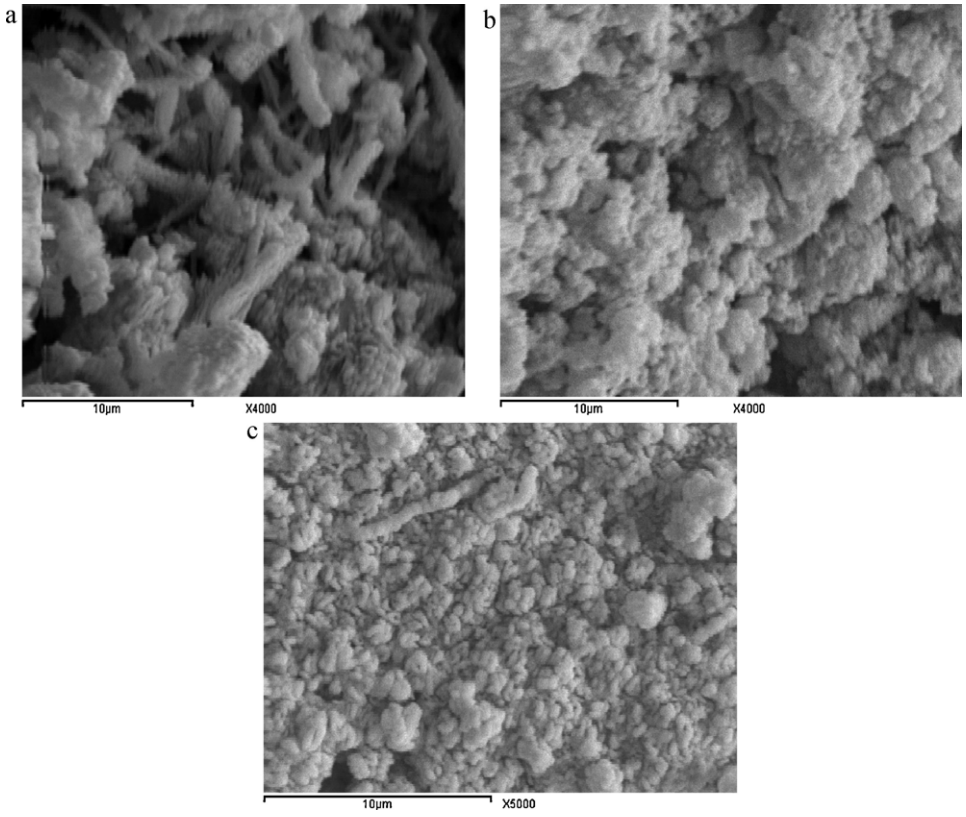

Fig. 8. The SEM images of HA sample (a) pre-immersion, (b) post-immersion for 7 days and (c) 28 days in SBF.

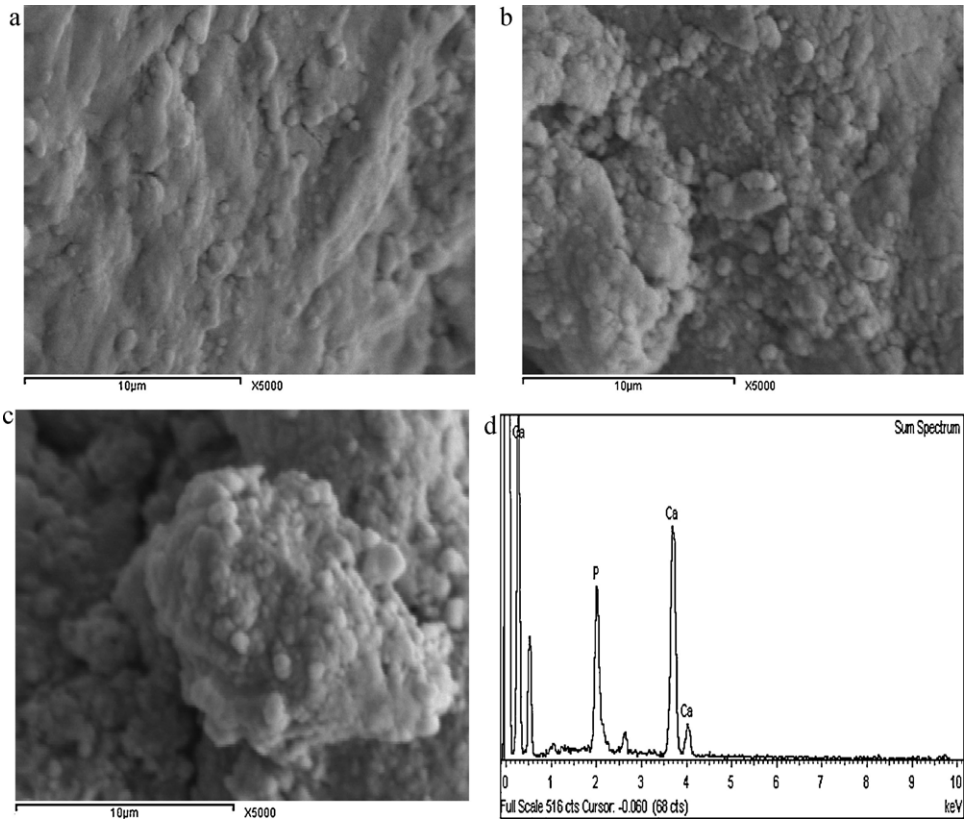

Fig. 9. The SEM images of C2 composite (a) pre-immersion, (b) post-immersion for 7 days and (c) 28 day in SBF and its EDAX analysis (d).

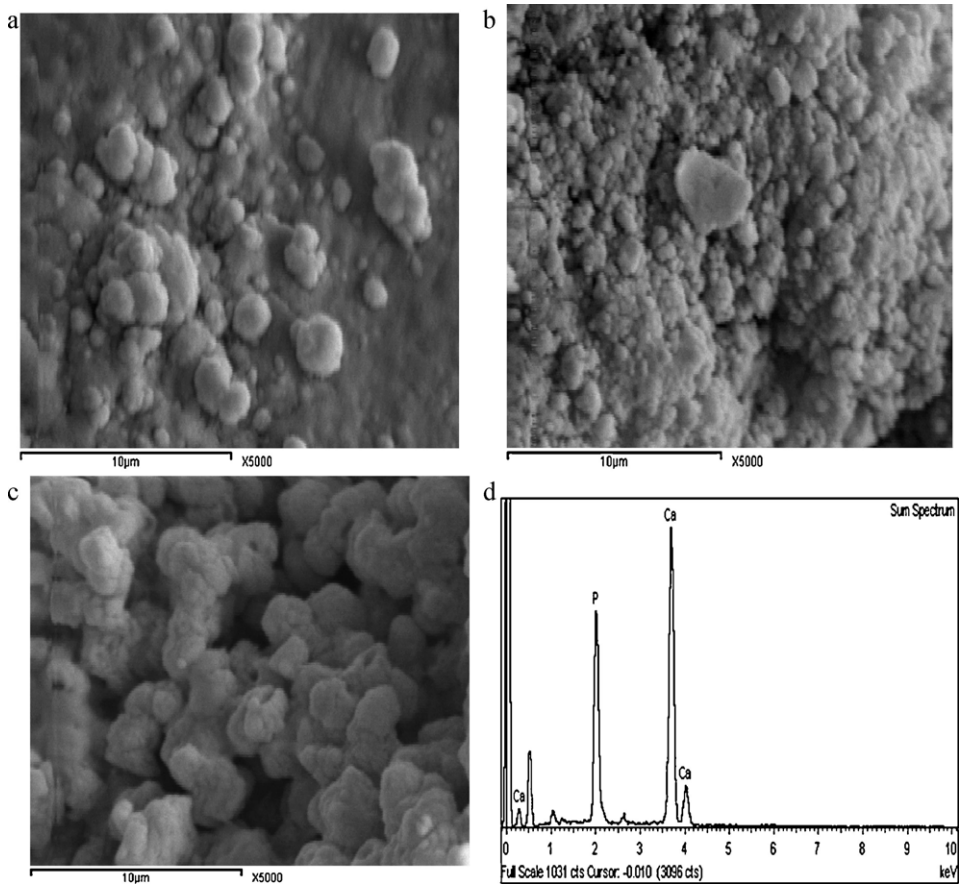

Fig. 10. The SEM images of C2·CA composite (a) pre-immersion, (b) post-immersion for 7 days, (c) 28 day in SBF and its EDAX analysis (d).

increase deposition of phosphate and carbonate ions onto the composite [17] (Fig. 7b). For C2·CA composite, the FT-IR results prove the decrease in the intensity of the HA bands such as OH, phosphate and carbonate groups post-immersion 7 and 28 days compared to pre-immersion confirming release of some ions from the composite (Fig. 7c).

3.1.2.4. Microstructure analysis. The SEM of prepared HA pre-immersion is composed of many white rods and few needle shapes proving CHA formation, which fused together forming clusters. The HA sample surface 7 days post-immersion has many spherical HA particles with growth of apatite crystals and many pores, while at 28 days, more and more HA particles are deposited, concentrated and covered the surface and the pores (Fig. 8). For C2 composite, 28 days post-immersion, there was a plenty of apatite crystals that deposited, accumulated and became large in size. Also, many pores formed and increased compared to 7 days due to high degradation of chitosan polymer [17] (Fig. 9).

The SEM photo of C2·CA composite surface pre-immersion shows smooth surface and many small spherical HA particles distributed and impeded into the composite structure. At 7 days, there is a lot of small and large spherical apatite particles deposited on it with many minute pores due to effect of immersion and some degradation of the polymer. At 28 days post-immersion, more and more apatite particles were present, increased in their size forming clusters and covered the pores in the composite as well as large pores were seen between the formed clusters (Fig. 10). In this domain, Junjie et al. [21] suggest that the ion/polar interactions are the main drive forces for nHCG formation via biomineralization. Also, the hydrogen bonds between OH, $–NH_2$ of chitosan in CG films and OH groups of HA crystals take the important role in the formation process of apatite layer.

In addition, elemental analysis (EDAX) of C2·CA composite 28 days post-immersion, show high Ca/P ratio (1.8) compared to C2 composite (1.45) proving vital role of CA in improvement of apatite formation precipitation (Figs. 9d and 10d).

4. Conclusion

The in vitro analysis proves the mineralization of Ca^{2+} and P ions onto nHA\chitosan composites containing high chitosan content proving chemical interaction. The CA addition proved high stability of the composites in SBF due to the interaction between HA particles. The hydrophilicity properties increased with increase of chitosan content but it decreased with CA addition because of interaction between HA, chitosan and CA. The deposition of spherical particles of apatite on the composites surface increased after addition of chitosan and more increased with CA. Therefore, the C2 and C2·CA composites can be applied for bone grafting and tissue engineering applications.

References

[1] J. Li, Y. Chen, Y. Yin, F. Yao, K. Yao, Modulation of nano-hydroxyapatite size via formation on chitosan-gelatin network film in situ, Biomaterials 28 (2007) 781–790.

[2] R. Murugan, S. Ramakrishna, Bioresorbable composite bone paste using polysaccharide based nanohydroxy apatite, Biomaterials 25 (2004) 3829–3835.

[3] N. Kivrak, A.C. Tas, Syntheses of calcium hydroxyapatite-tricalcium phosphate composite bioceramics powders and their sintering behavior, Am. Ceram. Soc. 81 (1998) 2245–2252.

[4] A. Burke, E. Yilmaz, N. Hasirci, O. Yilmaz, Iron removal from solution through adsorption on chitosan, Appl. Poly. Soc. 84 (2002) 1185.

[5] M. Ito, In-vitro properties of chitosan bonded hydroxyapatite bone filling paste, Biomaterials 12 (1991) 41.

[6] Y. Huang, S. Onyeri, M. Siewe, A. Moshfeghina, In vitro characterization of chitosan-gelatin scaffolds for tissue engineering, Biomaterials 26 (2005) 7616–7627.

[7] H. Bundela, A.K. Bajpai, Designing of hydroxyapatite-gelatin based porous matrix as bone substitutes: correlation with biocompatibility aspects, Polym. Lett. 2 (2008) 201–213.

[8] E.T. Baran, K. Tuzlakoglu, A.J. Salgado, R.L. Reis, Multichannel mould processing of 3D structures from micro porous coralline hydroxyapatite granules and chitosan support materials for guided tissue regeneration/engineering, Mater. Med. 15 (2004) 161–165.

[9] L. Zhang, L. Yubao, Y. Apiing, P. Xuelin, W. Xuejiang, Z. Xiang, Preparation and in-vitro investigation of chitosan/nano-hydroxyapatite composite used as bone substitute materials, Mater. Med. 16 (2005) 213–219.

[10] C. Xianmiao, L. Yubao, Z. Yi, Z. Li, L. Jidong, W. Huanan, Properties and in vitro biological evaluation of nano-hydroxyapatite/chitosan membranes for bone guided regeneration, Mater. Sci. Eng. C 29 (2009) 29–35.

[11] R. Murugan, S. Ramakrishna, Crystallographic study of Hydroxyapatite bioceramics derived from various sources, Cryst. Growth Des. 5 (2005) 111–112.

[12] S.H. Rhee, Tanaka, J. Am. Ceram. Soc. 81 (1998) 3029.

[13] S.H. Rhee, H. Tanaka, Hydroxyapatite formation on cellulose cloth induced by citric acid, J. Mater. Sci.: Mater. Med. 11 (2000) 449–452.

[14] R.T. Tran, P. Thevenot, Y. Zhang, D. Gyawali, L. Tang, J. Yang, Scaffold sheet design strategy for soft tissue engineering, Materials 2 (2010) 1375e89.

[15] T. Kokubo, H. Takadama, How useful is SBF in predicting in-vivo bone bioactivity? Biomaterials 27 (2006) 2907–2915.

[16] A.M. El-Kady, K.R. Mohamed, G.T. El-Bassyouni, Fabrication, characterization and bioactivity evaluation of calcium pyrophosphate/polymeric biocomposites, J. Ceram. Int. 35 (7) (2009) 2933–2942.

[17] R.K. Mohamed, G.T. El-Bassyouni, H.H. Al-Beheri, Chitosan graft copolymer-HA/DBM biocomposites: preparation, characterization and in-vitro evaluation, J. Appl. Polym. Sci. 105 (2007) 2553–2563.

[18] X. Shen, H. Tong, T. Jiang, Z. Zhu, P. Wan, J. Hu, Homogeneous chitosan/carbonate apatite/citric acid nanocomposites prepared through a novel in situ precipitation method, Compos. Sci. Technol. 67 (2007) 2238–2245.

[19] I. Yamaguchi, S. Iizuka, A. Osaka, H. Monma, J. Tanaka, The effect of citric acid addition on chitosan/hydroxyapatite composites, Colloids Surf. A: Physicochem. Eng. Aspect 214 (2003) 111–118.

[20] R.K. Mohamed, A.A. Mostafa, Preparation and bioactivity evaluation of hydroxyapatite-titania/chitosan-gelatin polymeric biocomposites, Mater. Sci. Eng. C 28 (2008) 1087–1099.

[21] L. Junjie, D. Yan, Y. Jun, Y. Yuji, Z. Hong, Y. Fanglian, W. Haibin, Y. Kangde, Surface characterization and biocompatibility of micro- and nano-hydroxyapatite/chitosan-gelatin network films, Mater. Sci. Eng. C 29 (2009) 1207–1215.